Cosmological evolution of global monopoles

Masahide Yamaguchi
Research Center for the Early Universe, University of Tokyo, Tokyo, 113-0033, Japan
(February 1, 2008)

We investigate the cosmological evolution of global monopoles in the radiation dominated (RD) and matter dominated (MD) universes by numerically solving field equations of scalar fields. It is shown that the global monopole network relaxes into the scaling regime, unlike the gauge monopole network. The number density of global monopoles is given by $n(t) \simeq (0.43 \pm 0.07)/t^3$ during the RD era and $n(t) \simeq (0.25 \pm 0.05)/t^3$ during the MD era. Thus, we have confirmed that density fluctuations produced by global monopoles become scale invariant and are given by $\delta\rho \sim 7.2(5.0)\sigma^2/t^2$ during the RD (MD) era, where σ is the breaking scale of the symmetry.

PACS: 98.80.Cq

Since Kibble pointed out that topological defects may have been formed as a consequence of cosmological phase transitions [1], many cosmological applications have been investigated [2]. In particular, the possibility is discussed that topological defects should become a source to produce density fluctuations responsible for the large-scale structure formation and the cosmic microwave background (CMB) anisotropy [2]. Recently, the BOOMERANG experiment [3] and the MAXIMA experiment [4] on observations of the CMB anisotropy revealed that our universe is flat, which is consistent with the prediction of inflation. However, they also found a relatively low second acoustic peak. One explanation of such a feature is a hybrid model, where primordial fluctuations are comprised of adiabatic fluctuations induced by inflation and isocurvature ones by topological defects [5]. In fact, topological defects are compatible with the inflationary scenario [6]. Moreover, deviations from Gaussianity in CMB are reported in [7]. Thus, it is still important to clarify the dynamics of topological defects and their implications on cosmology.

Among many types of topological defects, particular attention has been paid to strings. This is mainly because it is confirmed that both the local* [8] and the global string networks [10,11] relax into the scaling regime, where the number of infinite strings per horizon volume is a constant irrespective of cosmic time, so that density fluctuations produced by strings become scale invariant. Thus, strings have been examined as a possible source to produce density fluctuations responsible for the large-scale structure formation and the CMB anisotropy [2]. Furthermore, global strings have been discussed in the context of axion cosmology [10,12,13]. As the result of the breakdown of the global Peccei-Quinn (PQ) $U(1)$ symmetry, global strings (axionic strings) are formed. Then, axions emitted from axionic strings may significantly contribute to the present energy density so that they may play the role of the cold dark matter (CDM).

On the other hand, monopoles have been less investigated because the formation of local monopoles, generally speaking, leads to conflict with observation. If they are diluted by inflation [14], annihilated by the Langacker-Pi mechanism [15], or swept away by the domain wall [16], the problem can be evaded but local monopoles leave no imprint on cosmological evolution. Unlike strings, however, the evolution of monopoles has distinct features depending on whether they are local or global. In fact, the long range force works between global monopoles so that their annihilations are much more efficient than the local counterpart. Therefore, the global monopole network may go into the scaling regime, where the number of global monopoles per horizon volume is a constant irrespective of cosmic time [17–19].

Bennett and Rhie made the first numerical simulations and found the tendency that the number of global monopoles per horizon volume is a constant though they used the nonlinear σ model equation to evolve the scalar fields [18]. Later, Pen, Spergel, and Turok performed similar numerical simulations in both the nonlinear σ model approximation and the full potential [19]. (See also [20].) However, due to a lack of computer power, they can only run a few realizations so that the number of global monopoles per horizon volume still has large errors and the scaling property cannot be definitely confirmed. Also, as will be shown later, we must pay attention to the boundary effects, the grid size effects, and the total box size dependence. In fact, the monopole can disappear under the periodic boundary condition due to the boundary effects.

Now that we have sufficient computer power, we can solve the equation of motion of the scalar fields ϕ^a without any approximations and run many realizations in order to investigate and remove the boundary effects, the grid size effects, and the total box size dependence so that we can ascertain whether the global monopole network enters the scaling regime. If so, the number density of global monopoles is completely determined. In this paper, we report the result of our numerical simulations for the evolution of the global monopole network. Also, a simple analytic estimate is given.

*There are still discussions on the energy loss mechanism of local strings, gravitational wave radiation via the loop formation, or direct heavy particle emission [9].

As mentioned above, we directly solve the equation of motion for scalar fields in the expanding universe. Let us consider the following Lagrangian density for scalar fields $\phi^a(x)$ $(a = 1, 2, 3)$,

$$\mathcal{L}[\phi^a] = \frac{1}{2} g_{\mu\nu} \partial^\mu \phi^a \partial^\nu \phi^a - V_{\rm eff}[\phi^a, T], \tag{1}$$

where $g_{\mu\nu}$ is the flat Robertson-Walker metric and the effective potential $V_{\rm eff}[\phi^a, T]$ is given by

$$\begin{aligned} V_{\rm eff}[\phi^a, T] &= \frac{\lambda}{4}(\phi^2 - \sigma^2)^2 + \frac{5}{24}\lambda T^2 \phi^2, \\ &= \frac{\lambda}{4}(\phi^2 - \eta^2)^2 + \frac{\lambda}{4}(\sigma^4 - \eta^4). \end{aligned} \tag{2}$$

Here $\phi \equiv \sqrt{\phi^a \phi^a}$, $\eta \equiv \sigma\sqrt{1 - (T/T_c)^2}$, and $T_c \equiv \frac{2}{5}\sqrt{15}\sigma$ is the critical temperature. For $T > T_c$, the potential $V_{\rm eff}[\phi^a, T]$ has a minimum at the origin and the $O(3)$ symmetry is restored. On the other hand, for $T < T_c$, new minima $\phi = \eta$ appear and the symmetry is broken. In this case the phase transition is of second order.

Then, the equation of motion for ϕ^a in the expanding universe is given by

$$\begin{aligned} \ddot{\phi^a}(x) + 3H\dot{\phi^a}(x) - \frac{1}{R(t)^2}\nabla^2 \phi^a(x) \\ + \lambda[\phi^2(x) - \eta^2]\phi^a(x) = 0, \end{aligned} \tag{3}$$

where the dot represents time derivative and $R(t)$ is the cosmic scale factor. The Hubble parameter $H = \dot{R}(t)/R(t)$ and the cosmic time t are given by

$$\begin{aligned} H^2 &= \frac{4\pi^3}{45 m_{\rm pl}^2} g_* T^4, \quad t = \frac{1}{2H} \equiv \frac{\epsilon_{RD}}{T^2} \qquad \text{(for RD)}, \\ H^2 &= \alpha(T)\frac{4\pi^3}{45 m_{\rm pl}^2} g_* T^4, \quad t = \frac{2}{3H} \equiv \frac{\epsilon_{MD}}{T^{3/2}} \quad \text{(for MD)}, \end{aligned} \tag{4}$$

where $m_{\rm pl} = 1.2 \times 10^{19}$ GeV is the Planck mass, and g_* is the total number of degrees of freedom for the relativistic particles. For the MD case, we have defined $\alpha(T)$ $[\alpha(T) > 1]$ as $\alpha(T) \equiv \rho_{\rm mat}(T)/\rho_{\rm rad}(T) = \alpha_c(T_c/T)$, where $\rho_{\rm mat}(T)$ is the contribution to the energy density from nonrelativistic particles, $\rho_{\rm rad}(T)$ the contribution from relativistic particles at the temperature T, and $\alpha_c \equiv \rho_{\rm mat}(T_c)/\rho_{\rm rad}(T_c)$. We also define the dimensionless parameter ζ as

$$\begin{aligned} \zeta_{RD} &\equiv \frac{\epsilon_{RD}}{\sigma} = \left(\frac{45}{16\pi^3 g_*}\right)^{1/2} \frac{m_{\rm pl}}{\sigma} \qquad \text{(for RD)}, \\ \zeta_{MD} &\equiv \frac{\epsilon_{MD}}{\sigma^{1/2}} = \left(\frac{5\sqrt{15}}{6\alpha_c \pi^3 g_*}\right)^{1/2} \frac{m_{\rm pl}}{\sigma} \quad \text{(for MD)}. \end{aligned} \tag{5}$$

In our simulation, we take $\zeta_{RD,MD} = 10$ and 5 to investigate ζ dependence on the result.

We start the simulations at the temperature $T_i = 2T_c$, which corresponds to $t_i = t_c/4$ (RD) and $t_i = t_c/(2\sqrt{2})$ (MD). Since the $O(3)$ symmetry is restored at the initial time $(T_i > T_c)$, we adopt as the initial condition the thermal equilibrium state with the mass,

$$m = \sqrt{\frac{5}{12}\lambda(T_i^2 - T_c^2)}, \tag{6}$$

which is the inverse curvature of the potential at the origin at $t = t_i$.

Hereafter we normalize the scalar field in units of t_i^{-1}, t and x in units of t_i, λ is set to be $\lambda = 0.25$, and the scale factor $R(t)$ is normalized as $R(1) = 1$.

We perform numerical simulations in seven different sets of lattice sizes and spacings for the RD case and the MD case (See Tables I and II.). In all cases, the time step is taken as $\delta t = 0.01$. In the typical case (1), the box size is nearly equal to horizon volume $(H^{-1})^3$ and the lattice spacing to a typical core size of a monopole $\delta x \sim 1.0/(\sqrt{\lambda}\sigma)$ at the final time t_f. Furthermore, in order to investigate the dependence of ζ, we arrange case (7) with $\zeta = 5$. We have simulated the system from 10 [(2), (3), (5) and (6)] or 50 [(1), (4), and (7)] different thermal initial conditions. Also, in order to investigate the effect of the boundary condition (BC), we adopt the periodic BC and the reflective BC [$\nabla^2 \phi^a(x) = 0$ on the boundary].

In order to judge whether the global monopole network relaxes into the scaling regime, we give time development of ξ, which is defined as

$$\xi \equiv n(t) t^3, \tag{7}$$

where $n(t)$ is the number density of global monopoles. Before counting the number of global monopoles in the simulation box, we must identify global monopoles. We introduce two identification methods. In one method (I), we use a static spherically symmetric solution, which is obtained by solving the equation

$$\frac{d^2\phi}{dr^2} + \frac{2}{r}\frac{d\phi}{dr} - 2\frac{\phi}{r^2} - \frac{dV_{\rm eff}[\phi, T]}{d\phi} = 0, \tag{8}$$

where $\phi^a(r, \theta, \varphi) \equiv \phi(r) x^a/r$ with $x^1 = r\sin\theta\cos\varphi, x^2 = r\sin\theta\sin\varphi, x^3 = r\cos\theta$, and the winding number $n = 1$. The boundary conditions are given by

$$\begin{aligned} &\phi(r) \to \eta, \qquad (r \to \infty), \\ &\phi(0) = 0. \end{aligned} \tag{9}$$

Since spacetime is discretized in our simulations, a point with $\phi = 0$ corresponding to a monopole core is not necessarily situated at a lattice point. In the worst case, a point with $\phi = 0$ lies at the center of a cube. We require that a lattice is identified with a monopole core if the potential energy density there is larger than that corresponding to the field value of a static spherically symmetric solution at $r = \sqrt{3}\delta x_{\rm phys}/2$ $[\delta x_{\rm phys} = R(t)\delta x]$. Moreover, in order to reduce the error, we regard the identified lattices which are connected as one monopole

core. In the other method (II), a cubic box is identified to include a monopole if all $\phi^a = 0$ ($a = 1, 2, 3$) surfaces pass through the cubic box. In this method, we also regard the identified boxes which are connected as one monopole core. In fact, as shown later, the results with these two identification methods coincide very well.

As an example, time development of ξ_{RD} in cases (1) to (6) under the periodic BC for the RD case is described in Fig. 1. We find that after some relaxation period, ξ_{RD} becomes a constant irrespective of time for all cases. Though all are consistent within the standard deviation, ξ_{RD} tends to increase as the box size does. This is because monopoles annihilate more often than those in the real universe under the periodic BC so that monopoles annihilate too much for smaller box sizes. On the other hand, under the reflective BC, we also find that ξ_{RD} becomes a constant irrespective of time after some relaxation period. ξ_{RD} is listed in Table I. In this case, contrary to the case under the periodic BC, ξ_{RD} tends to decrease as the box size increases. This is because a monopole suffers a repulsive force from the boundary so that monopoles near the boundary annihilate less often and ξ_{RD} takes larger values in smaller-box simulations due to the boundary effect. Therefore, the real number of the monopole per horizon volume lies in between those under the periodic and the reflective BC. From the results of the largest-box simulations [case (6)], we conclude that ξ_{RD} converges to a constant $\xi_{RD} \simeq 0.43 \pm 0.07$ irrespective of the boundary conditions. Therefore we can conclude that the global monopole network relaxes into the scaling regime in the RD universe. We also show time development of ξ_{RD} in case (7) under the periodic BC in Fig. 2. First of all, as easily seen, the results with two identification methods agree very well. Next, ξ_{RD} asymptotically becomes a constant, 0.36 ± 0.01, which is consistent with all the above cases with $\zeta = 10$ within the standard deviation. Hence we can also conclude that ζ does not change the essential result.

For the MD case, we also find that after some relaxation period, the number of global monopoles per horizon volume becomes a constant irrespective of cosmic time under the periodic BC expect for cases (1), (2), and (3), in which global monopoles annihilate too much due to the boundary effect. The trend of the boundary effect is the same as that for the RD case. Therefore, from the results of the largest-box simulations [case (6)], we conclude that ξ_{MD} converges to a constant $\xi_{MD} \simeq 0.25 \pm 0.05$ irrespective of the boundary conditions. Thus, we have completely confirmed that the global monopole network goes into the scaling regime in both the RD and MD universes.

The above results can be understood by the following simple discussion. The evolution of the number density of global monopoles $n(t)$ is described by the Boltzmann equation,[†]

$$\frac{dn(t)}{dt} = -P(t)n(t) - 3H(t)n(t), \\ = -\frac{n(t)}{T(t)} - \frac{3mn(t)}{t}, \tag{10}$$

where $R(t) \propto t^m$, $P(t)$ is the probability per unit time that a monopole annihilates with an antimonopole, and $T(t)$ is the period it takes for a pair of monopoles at rest with the mean separation $l(t)$ to pair annihilate. The mean separation $l(t)$ is given by $l(t) \equiv R(t) r_s = n(t)^{-1/3}$, where r_s is the mean comoving separation. Since a constant attractive force works between a pair of monopoles irrespective of the separation length, we assume that the relative velocity between them reaches unity at once and that they do not spiral around each other for a long period of time. Then, the period $T(t)$ is given by the following relation,

$$\int_{t_0}^{T+t_0} \frac{dt}{R(t)} = \int_0^{r_s} dr, \tag{11}$$

where t_0 is the initial time where a pair of monopoles are at rest. Then, the period $T(t)$ reads

$$T(t) \simeq \frac{1-m}{n(t)^{1/3}}, \qquad (\text{for } \ t_0 \ll T). \tag{12}$$

Inserting this into the Eq. (10), the number density $n(t)$ takes the following asymptotic value,

$$n(t) \simeq \frac{27(1-m)^6}{t^3} \propto t^{-3}. \tag{13}$$

From the above asymptotic form, we find that $n_{RD}(t) \simeq 0.42/t^3$ and $n_{MD}(t) \simeq 0.04/t^3$. For the RD case, $n(t)$ for the simulation and the analytic estimate agrees excellently up to the proportional coefficient ξ_{RD}. The difference of the proportional coefficient ξ_{MD} between the simulation and the analytic estimate may come from the fact that cosmic expansion is so rapid in the matter dominated universe that our assumption that the relative velocity between them reaches unity at once breaks down to some extent.

We summarize our results. By directly solving equations of motion for scalar fields in the expanding universe, we have confirmed that the global monopole network enters the scaling regime in both the RD and MD universes. The number density of global monopoles is given by $n(t) = (0.43 \pm 0.07)/t^3$ for the RD case and $n(t) = (0.25 \pm 0.05)/t^3$ for the MD case. Then, density fluctuations induced by global monopoles are given by $\delta\rho \simeq m(t)n(t)/t^3 \sim 7.2(5.0)\sigma^2/t^2$ for the RD (MD) era,

[†]A similar discussion was done in [21] in the 2+1 dimension.

where $m(t) \simeq 4\pi\sigma^2 n^{-1/3}(t) \propto t$ is the mass of a global monopole.

The author is grateful to J. Yokoyama for useful comments. This work was partially supported by the Japanese Grant-in-Aid for Scientific Research from the Ministry of Education, Culture, Sports, Science, and Technology.

[1] T. W. B. Kibble, J. Phys. A **9**, 1387 (1976).
[2] See, for a review, A. Vilenkin and E. P. S. Shellard, *Cosmic String and Other Topological Defects* (Cambridge University Press, Cambridge, England, 1994).
[3] P. de Bernardis *et al.*, Nature (London) **404**, 955 (2000); A. E. Lange *et al.*, Phys. Rev. D **63**, 042001 (2001).
[4] S. Hanany *et al.*, Astrophys. J. Lett. **545**, L5 (2000); A. Balbi *et al.*, *ibid.* **545**, L1 (1900).
[5] F. R. Bouchet, P. Peter, A. Riazuelo, and M. Sakellariadou, astro-ph/0005022; C. R. Contaldi, astro-ph/0005115.
[6] J. Yokoyama, Phys. Rev. Lett. **63**, 712 (1989); Phys. Lett. B **212**, 273 (1988).
[7] P .G. Ferreira, J. Magueijo, and K. M. Gorski, Astrophys. J. Lett. **503**, L1 (1998); J. Pando, D. Valls-Gabaud, and L. Fang, Phys. Rev. Lett. **81**, 4568 (1998); D. Novikov, H. Feldman, and S. Shandarin, Int. J. Mod. Phys. D **8**, 291 (1999).
[8] A. Albrecht and N. Turok, Phys. Rev. Lett. **54**, 1868 (1985); Phys. Rev. D **40**, 973 (1989); D. P. Bennett and F. R. Bouchet, Phys. Rev. Lett. **60**, 257 (1988); **63**, 2776 (1989); Phys. Rev. D **41**, 2408 (1990); B. Allen and E. P. S. Shellard, Phys. Rev. Lett. **64**, 119 (1990).
[9] G. R. Vincent, M. Hindmarsh, and M. Sakellariadou, Phys. Rev. D **56**, 637 (1997); G. R. Vincent, N. D. Antunes, and M. Hindmarsh, Phys. Rev. Lett. **80**, 2277 (1998).
[10] M. Yamaguchi, M. Kawasaki, and J. Yokoyama, Phys. Rev. Lett. **82**, 4578 (1999).
[11] M. Yamaguchi, Phys. Rev. D **60**, 103511 (1999); M. Yamaguchi, M. Kawasaki, and J. Yokoyama, *ibid.* **61**, 061301 (2000).
[12] R. L. Davis, Phys. Rev. D **32**, 3172 (1985); Phys. Lett. B **180**, 225 (1986); R. L. Davis and E. P. S. Shellard, Nucl. Phys. **B324**, 167 (1989); A. Dabholkar and J. M. Quashnock, *ibid.* **333**, 815 (1990); R. A. Battye and E. P. S. Shellard, *ibid.* **423**, 260 (1994); Phys. Rev. Lett. **73**, 2954 (1994).
[13] D. Harari and P. Sikivie, Phys. Lett. B **195**, 361 (1987); C. Hagmann and P. Sikivie, Nucl. Phys. **B363**, 247 (1991); C. Hagmann, S. Chang, and P. Sikivie, Phys. Rev. D **63**, 125015 (2001).
[14] See, for example, A. D. Linde, *Particle Physics and Inflationary Cosmology* (Harwood, Chur, Switzerland, 1990).
[15] P. Langacker and S.-Y. Pi, Phys. Rev. Lett. **45**, 1 (1980).
[16] G. Dvali, H. Liu, and T. Vachaspati, Phys. Rev. Lett. **80**, 2281 (1998).
[17] M. Barriola and A. Vilenkin, Phys. Rev. Lett. **63**, 341 (1989).
[18] D. P. Bennett and S. H. Rhie, Phys. Rev. Lett. **65**, 1709 (1990).
[19] U. Pen, D. N. Spergel, and N. Turok, Phys. Rev. D **49**, 692 (1994).
[20] M. Kunz and R. Durrer, Phys. Rev. D **55**, R4516 (1997), R. Durrer, M. Kunz, and A. Melchiorri, *ibid.* **59**, 123005 (1999).
[21] M. Yamaguchi, J. Yokoyama, and M. Kawasaki, Prog. Theor. Phys. **100**, 535 (1998).

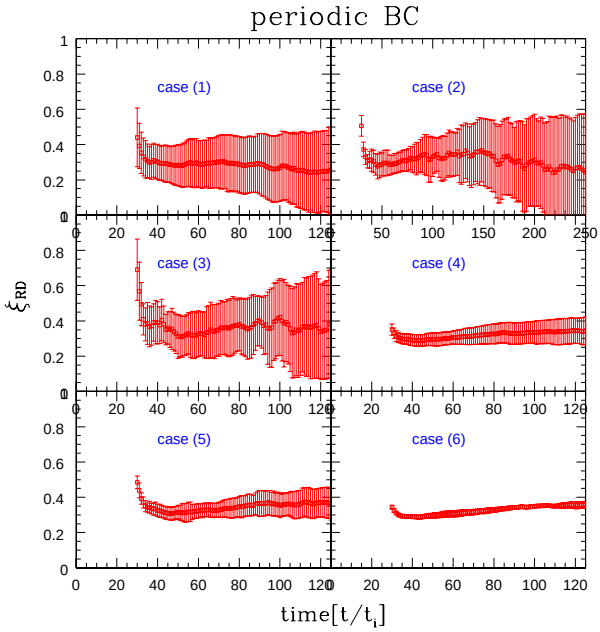

FIG. 1. Time development of ξ_{RD} in cases (1) to (6) under the periodic BC for the RD case. Symbols (□) represent time development of ξ_{RD}. The vertical lines denote a standard deviation over different initial conditions.

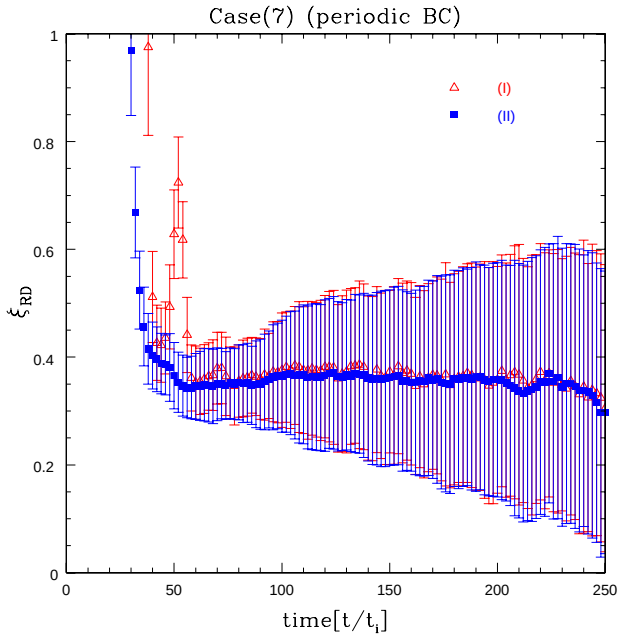

FIG. 2. Time development of ξ_{RD} in case (7) under the periodic BC for the RD case. Filled squares represent time development of ξ_{RD} for identification method (I) using the spherical symmetric solution, blank triangles for that (II) using the $\phi^a = 0$ surface. The vertical lines denote a standard deviation over different initial conditions.

TABLE I. Seven different sets of simulations for the RD case.

Case	Lattice number	Lattice spacing (δx) [unit = $t_i R(t)$]	ζ	Realization	Box size/H^{-1} (at final time)	ξ (periodic BC)	ξ (reflective BC)
(1)	128^3	$\sqrt{3}/10$	10	50	1 (at 125)	0.28 ± 0.19	1.00 ± 035
(2)	256^3	$\sqrt{6}/20$	10	10	1 (at 250)	0.31 ± 0.20	0.83 ± 0.15
(3)	256^3	$\sqrt{3}/20$	10	10	1 (at 125)	0.35 ± 0.21	0.71 ± 0.33
(4)	128^3	$\sqrt{3}/5$	10	50	2 (at 125)	0.37 ± 0.06	0.71 ± 0.11
(5)	256^3	$\sqrt{3}/10$	10	10	2 (at 125)	0.36 ± 0.07	0.58 ± 0.12
(6)	256^3	$\sqrt{3}/5$	10	10	4 (at 125)	0.36 ± 0.01	0.50 ± 0.03
(7)	128^3	$\sqrt{6}/10$	5	50	1 (at 250)	0.36 ± 0.17	0.61 ± 0.21

TABLE II. Seven different sets of simulations for the MD case.

Case	Lattice number	Lattice spacing (δx) [unit = $t_i R(t)$]	ζ	Realization	Box size/H^{-1} (at final time)	ξ (periodic BC)	ξ (reflective BC)
(1)	128^3	$3(100)^{1/3}/256$	10	50	1 (at 100)	Disappearance	0.75 ± 0.36
(2)	256^3	$3(200)^{1/3}/512$	10	10	1 (at 200)	Disappearance	0.77 ± 0.10
(3)	256^3	$3(100)^{1/3}/512$	10	10	1 (at 100)	Disappearance	0.82 ± 0.50
(4)	128^3	$3(100)^{1/3}/128$	10	50	2 (at 100)	0.19 ± 0.09	0.42 ± 0.10
(5)	256^3	$3(100)^{1/3}/256$	10	10	2 (at 100)	0.21 ± 0.09	0.41 ± 0.05
(6)	256^3	$3(100)^{1/3}/128$	10	10	4 (at 100)	0.20 ± 0.02	0.30 ± 0.02
(7)	128^3	$3(200)^{1/3}/256$	5	50	1 (at 200)	Disappearance	0.44 ± 0.03